Fabrication of Magnetic Luminescent Nanocomposites by a Layer-by-Layer Self-assembly Approach

Xia Hong,[†] Jun Li,[†] Meijia Wang,[‡] Jinjie Xu,[†] Wei Guo,[†] Jinghong Li,*[,‡,§] Yubai Bai,*[,†] and Tiejin Li[†]

College of Chemistry, Jilin University, Changchun 130023, P. R. China, State Key Laboratory of Electroanalytical Chemistry, Changchun Institute of Applied Chemistry, Chinese Academy of Sciences, Changchun 130022, P. R. China, and Department of Chemistry, Tsinghua University, Beijing 100084, P. R. China

Received April 6, 2004. Revised Manuscript Received June 14, 2004

Magnetic luminescent nanocomposites were prepared via a layer-by-layer (LbL) assembly approach. The Fe_3O_4 magnetic nanoparticles of 8.5 nm were used as a template for the deposition of the CdTe quantum dots (QDs)/polyelectrolyte (PE) multilayers. The number of polyelectrolyte multilayers separating the nanoparticle layers and the number of QDs/polyelectrolyte deposition cycles were varied to obtain two kinds of magnetic luminescent nanocomposites, Fe_3O_4/PE_n/CdTe and Fe_3O_4/$(PE_3/CdTe)_n$, respectively. The assembly processes were monitored through microelectrophoresis and UV−vis spectra. The topography and the size of the nanocomposites were studied by transmission electron microscopy. The LbL technique for fabricating magnetic luminescent nanocomposites has some advantages to tune their properties. It was found that the selection of a certain number of the inserted polyelectrolyte interlayers and the CdTe QDs loading on the nanocomposites could optimize the photoluminescence properties of the nanocomposites. Furthermore, the nanocomposites could be easily separated and collected in an external magnetic field. It provides a novel technological innovation for luminescent tagging applications in biomedicine and biotechnology, such as rapid, convenient separation in vitro or site-specific transport in vivo due to the excellent magnetic properties of the nanocomposites.

Introduction

In the past decade, colloidal II−VI semiconductor nanocrystals, often referred to as "quantum dots" or QDs, have gained increasing attention in technological applications and fundamental studies due to their unique optical properties.[1−5] The nanocrystals exhibit size-dependent tunable photoluminescence (PL) with narrow emission bandwidths that span the visible spectrum, as well as broad absorption spectra that allow simultaneous efficient excitation of all colors of QDs at a single wavelength.[6−10] Also, they have high quantum yield and excellent photostability.[11,12] Such advantages over conventional organic dyes make it possible to become a new class of luminescent probes for biological and biomedical applications. Alivisatos and co-workers[13] and Chan and Nie.[14] first reported the use of QD conjugates for labeling biological specimens. Subsequently, Nie and co-workers[15] incorporated multicolor QDs into polystyrene microbeads for multiplex optical coding of biomolecules. More recently, the QDs with four different surface coatings were successfully used in in vivo imaging by Ballou et al.[16]

Magnetic nanoparticles, e.g., Fe_3O_4, are additional important materials due to their interesting magnetic properties and have been sophisticatedly employed in many advanced technology areas, including biology, pharmacy, and diagnostics.[17−24] For example, the magnetic labeled biological materials were rapidly, conve-

* To whom correspondence should be addressed. Prof. Y. Bai: phone, 86-431-8499192; fax, 86-431-8949334; e-mail, yubai@jlu.edu.cn. Prof. J. Li: phone, 86-431-5262243; fax, 86-431-5262243; e-mail, lijingh@ciac.jl.cn.
[†] Jilin University.
[‡] Chinese Academy of Sciences.
[§] Tsinghua University.

(1) Alivisatos, A. P. *Science* **1996**, *271*, 933.
(2) Klimov, V. L.; Mikhailovsky, A. A.; Xu, S.; Malko, A.; Hollingsworth, J. A.; Leatherdale, C. A.; Eisler, H. J.; Bawendi, M. G. *Science* **2000**, *290*, 314.
(3) Peng, X. G.; Manna, L.; Yang, W. D.; Wickham, J.; Scher, E.; Kadavanich, A.; Alivisatos, A. P. *Nature* **2000**, *404*, 59.
(4) Battaglia, D.; Peng, X. G. *Nano Lett.* **2002**, *2*, 1027.
(5) Cao, Y. W.; Banin, U. *J. Am. Chem. Soc.* **2000**, *122*, 9692.
(6) Schlamp, M. C.; Peng, X. G.; Alivisatos, A. P. *J. Appl. Phys.* **1997**, *82*, 5837.
(7) Mattoussi, H.; Radzilowski, L. H.; Dabbousi, B. O.; Thomas, E. L.; Bawendi, M. G.; Rubner, M. F. *J. Appl. Phys.* **1998**, *83*, 7965.
(8) Rodriguez-Viejo, J.; Mattoussi, H.; Heine, J. R.; Kuno, M. K.; Michel, J.; Bawendi, M. G.; Jensen, K. F. *J. Appl. Phys.* **2000**, *87*, 8526.
(9) Hines, M. A.; Guyot-Sionnest, P. *J. Phys. Chem.* **1996**, *100*, 468.
(10) Dabbousi, B. O.; Rodrigez-Viejo, J.; Mikulec, F. V.; Heine, J. R.; Mattoussi, H.; Ober, R.; Jensen, K. F.; Bawendi, M. G. *J. Phys. Chem. B* **1997**, *101*, 9463.
(11) Spanhel, L.; Haase, M.; Weller, H.; Henglein, A. *J. Am. Chem. Soc.* **1987**, *109*, 5649.
(12) Peng, X.; Schlamp, M. C.; Kadavanich, A. V.; Alivisatos, A. P. *J. Am. Chem. Soc.* **1997**, *119*, 7019.
(13) Bruchez, M., Jr.; Moronne, M.; Gin, P.; Weiss, S.; Alivisatos, A. P. *Science* **1998**, *281*, 2013.
(14) Chan, W. C. W.; Nie, S. *Science* **1998**, *281*, 2016.
(15) Han, M.; Gao, X.; Su, J. Z.; Nie, S. *Nat. Biotechnol.* **2001**, *19*, 631.
(16) Baullou, B.; Lagerholm, B. C.; Ernst, L. A.; Bruchez, M. P.; Waggoner, A. S. *Bioconjugate Chem.* **2004**, *15*, 79.
(17) Mosbach, K.; Anderson, L. *Nature* **1977**, *270*, 259.
(18) Miltenyi, S.; Müller, W.; Weichel, W.; Radbruch, A. *Cytometry* **1990**, *11*, 231.
(19) Doyle. P.; Bibette, J.; Bancaud, A.; Viovy, J. *Science* **2002**, *295*, 2237.

10.1021/cm049422o CCC: $27.50
Published on Web 09/15/2004

niently, and efficiently separated in an external magnetic field.[17,18] In a targeting drug-delivery system, the magnetic labeling of drugs could be easily administered and transported to the terminal under the guidance of an external magnetic field, leading to a safer and more effective tissues-specific release of drugs.[20] Magnetic nanoparticles combined with semiconductor nanocrystals would lead to a special functionalized magnetic luminescent composite that enjoys both the advantages of magnetic nanoparticles and semiconductor QDs and offers higher potential applications. Wang et al.[25] used dimercapto-succinimid acid modified γ-Fe_2O_3 nanoparticles reacted with CdSe/ZnS QDs to prepare water-soluble magnetic luminescent composites in an organic/water two-phase mixture. Through immobilized anticycline E antibodies on the surface, the breast cancer cells in serum were successfully separated and detected. Gaponik et al.[26] simultaneously encapsulated both CdTe QDs and Fe_3O_4 in polymer microcapsules to prepare a magnetic luminescent composite. They thought these multifunctional water-soluble capsules could be used for controlled release and directed drug delivery.

In this paper, we employed the layer-by-layer (LbL) approach to prepare magnetic luminescent nanocomposites. The LbL approach was based on the electrostatic attraction between the oppositely charged species deposited. The major advantage is that it permits the preparation of coated colloids of different shapes and sizes, with uniform layers of diverse composition as well as controllable thickness.[27−32] The Fe_3O_4 nanoparticles were used as a template for the deposition of polyelectrolyte multilayers/CdTe QDs (i.e., Fe_3O_4/PE_n/CdTe) or alternative adsorption of three polyelectrolyte layers/CdTe QDs multilayers (i.e., Fe_3O_4/$(PE_3/CdTe)_n$). The reason to use the CdTe QDs was that it was an important member of the II−VI semiconductor nanocrystals and could be synthesized in aqueous solution with strong photoluminescence.[33−37] In is well-known that water solubility is crucial to most biological applications. Either the distance between the Fe_3O_4 nanoparticles and the CdTe QDs or the number of alternative deposited PE_3/CdTe QDs multilayers could be controlled precisely by the LbL approach, resulting in determination of the PL of the nanocomposites. Moreover, the nanocomposites have excellent magnetic properties and can be conveniently separated and collected in an external magnetic field. They could be utilized in the fields of biolabeling, bioseparation, immunoassay, and various other diagnostic applications.

Experimental Section

Materials. Poly(allylamine hydrochloride) (PAH, M_w 8000−11000), α,α,α-tris(hydroxymethyl)methylamine (Tris), ferric chloride, ferrous chloride, cadmium perchlorate hydrate, and tetramethylammonium hydroxide were obtained from Aldrich. Poly(sodium 4-styrenesulfonate) (PSS, M_w 13400) was purchased from Fluka. Tellurium (reagent powder) and thioglycolic acid (TGA) were purchased from Acros. Milli-Q water (18.3 MΩ·cm^{-1}) was used as a solvent.

Synthesis of Fe_3O_4 Nanoparticles. The Fe_3O_4 nanoparticles were prepared by Massart's method.[38] In a typical experiment, a mixed aqueous solution of ferric chloride (50 mL, 1 M) and ferrous chloride (10 mL, 2 M, in 2 M HCl) were added slowly into ammonia solution (500 mL, 0.7 M) under vigorous stirring for 30 min at room temperature in a nitrogen atmosphere. The resulting black precipitates were collected by a permanent magnet. An aqueous solution of 1 M tetramethylammonium hydroxide and 3 mg of adipic acid were added to the precipitates. The solution reacted overnight at room temperature. Then the precipitates were separated from the solution by a permanent magnet and redispersed in 20 mM of Tris containing 20 mM NaCl. The concentration of the colloidal solution was about 25 mM.

Synthesis of TGA-Capped CdTe QDs. The CdTe QDs were prepared following the modified method by adding Cd^{2+} into a NaHTe solution in the presence of thioglycolic acid (TGA).[33,39] In brief, 12 mmol of TGA was added to a solution of 5 mmol of $Cd(ClO_4)_2 \cdot 6H_2O$ in 200 mL of water in a three-necked flask. Then the solution was adjusted to pH 11 with 1 M NaOH and deaerated with N_2 for 30 min. After that, 2.5 mmol of oxygen-free NaHTe solution was injected into the three-necked flask under vigorous stirring, which was freshly prepared from tellurium powder and $NaBH_4$ (molar rate of 1:2) in water. The resulting mixtures were then subjected to reflux for 12 h.

Fabrication of Fe_3O_4/PE_n/CdTe Nanocomposites. A 0.2-mL aliquot of 10 mg ml^{-1} of PAH aqueous solution containing 20 mM Tris and 20 mM NaCl was added to 1 mL of the negatively charged Fe_3O_4. The PAH was allowed to adsorb for 20 min under stirring. PAH-coated Fe_3O_4 nanoparticles were then collected by magnetic separation, followed by washing with 20 mM Tris aqueous containing 20 mM NaCl several times. Finally, they were redispersed in 1 mL of the identical Tris solution and sonicated for 10 min to prevent aggregation. Negatively charged PSS was then deposited onto the coated Fe_3O_4 nanoparticles in the same conditions and procedures. The above processes were repeated until the desired number of PAH/PSS layers was deposited (see Scheme 1). Then 3 mL of the negatively charged CdTe QDs was added to 1 mL of PE_n-coated Fe_3O_4 solution with an outermost layer of positively charged PAH. The composites were allowed to equilibrate overnight under stirring. The excess CdTe QDs were subsequently removed by three magnetic separation/redispersion cycles.

(20) Morimoto, Y.; Okumura, M.; Sugibayashi, K.; Kato, Y. *J. Pharm. Dyn.* **1981**, *4*, 624.
(21) Josephson, L.; Perea, J. M.; Weissleder, R. *Angew. Chem., Int. Ed.* **2001**, *40*, 3204.
(22) Hoehn, M.; Küstermann, E.; Blunk, J.; Wiedermann, D.; Trapp, T.; Wecker, S.; Föcking, M.; Arnold, H.; Hescheler, J.; Fleischmann, B. K.; Schwindt, W., Bührle, C. *Proc. Natl. Acad. Sci. U.S.A.* **2002**, *99*, 16267.
(23) Ito, A.; Shinkai, M.; Honda, H.; Kobayashi, T. *Cancer Gene Ther.* **2001**, *8*, 649.
(24) Shinkai, M. *J. Biosci. Bioeng.* **2002**, *94*, 606.
(25) Wang, D.; He, J.; Rosenzweig, N.; Rosenzweig, Z. *Nano Lett.* **2004**, *4*, 409.
(26) Gaponik, N.; Radtchenko, I. L.; Sukhorukov, G. B.; Rogach, A. L. *Langmuir* **2004**, *20*, 1449.
(27) Decher, G.; Hong, J. D. *Ber. Bunsen-Ges. Phys. Chem.* **1991**, *95*, 1430.
(28) Decher, G. *Science* **1997**, *277*, 1232.
(29) Caruso, F.; Caruso, R. A.; Möhwald, H. *Science* **1998**, *282*, 1111.
(30) Caruso, F.; Susha, A. S.; Giersig, M.; Möhwald, H. *Adv. Mater.* **1999**, *11*, 950.
(31) Wang, D.; Rogach, A. L.; Caruso, F. *Nano Lett.* **2002**, *2*, 857.
(32) Kulakovich, O.; Strekal, N.; Yaroshevich, A.; Maskevich, S.; Gaponenko, S.; Nabiev, I.; Woggon, U.; Artemyev, M. *Nano Lett.* **2002**, *2*, 1449.
(33) Gaponik, N.; Talapin, D. V.; Rogach, A. L.; Hoppe, K.; Shevchenko, E. V.; Kornowski, A.; Eychmüller, A.; Weller, H. *J. Phys. Chem. B* **2002**, *106*, 7177.
(34) Rockenberger, J.; Tröger, L.; Rogach, A. L.; Tischer, M.; Grundmann, M.; Eychmüller, A.; Weller, H. *J. Phys. Chem. B* **1998**, *102*, 7807.
(35) Kapitonov, A. M.; Stupak, A. P.; Gaponenko, S. V.; Petrov, E. P.; Rogach, A. L.; Eychmüller, A. *J. Phys. Chem. B* **1999**, *103*, 10109.
(36) Rogach, A. L.; Katsikas, L.; Kornowski, A.; Su, D.; Eychmüller, A.; Weller, H. *Ber. Bunsen-Ges. Phys. Chem.* **1996**, *100*, 1772.
(37) Gao, M.; Kirstein, S.; Möhwald, H.; Rogach, A. L.; Kornowski, A.; Eychmüller, A.; Weller, H. *J. Phys. Chem. B* **1998**, *102*, 8360.
(38) Massart, R. *IEEE Trans. Magn.* **1981**, *17*, 1247.
(39) Zhang, H.; Zhou, Z.; Yang, B. *J. Phys. Chem. B* **2003**, *107*, 8.

Scheme 1. Schematic Illustration of the LbL Process Forming the Magnetic Luminescent Nanocomposites

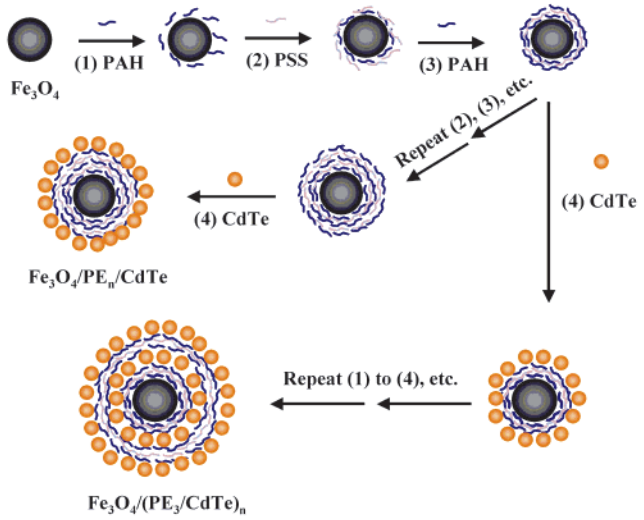

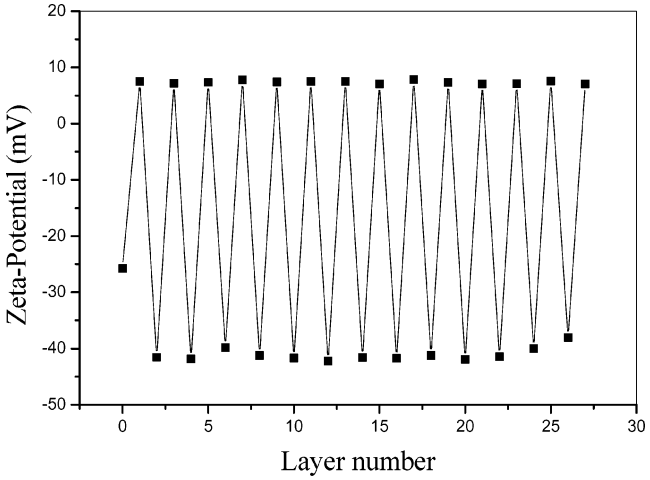

Figure 1. Zeta-potential of the negatively charged Fe_3O_4/PE_n nanoparticles as a function of polyelectrolyte layer number for PAH/PSS coatings. The odd layer numbers correspond to PAH deposition and the even layer numbers to PSS adsorption.

Fabrication of $Fe_3O_4/(PE_3/CdTe)_n$ Nanocomposites. Prior to the deposition of the CdTe QDs layer, the primer three polyelectrolyte layers (PAH/PSS/PAH, PE_3) were formed by alternative adsorption of PAH and PSS (0.2 mL from 10 mg mL^{-1} solution containing 20 mM Tris aqueous containing 20 mM NaCl) onto 1 mL of negatively charged Fe_3O_4 nanoparticles, as described above. The polyelectrolyte adsorption time was 20 min. After each adsorption step, the excess polyelectrolyte was removed by three repeated magnetic separation/wash/redispersion cycles. The CdTe QDs coatings on the Fe_3O_4 nanoparticles was done by adding 3 mL of the negatively charged CdTe QDs into 1 mL of PE_3-coated Fe_3O_4 solution, sitting overnight for QDs adsorption, removing excess QDs by three magnetic separation/redispersion cycles, and subsequently depositing another PE_3 layers, as outlined above for the prime layers. The processes were repeated until the desired number of CdTe QDs/PE_3 layers was formed.

Characterization. Transmission electron microscopy (TEM) measurements were performed with a JEOL-2010 microscope operated at an acceleration voltage of 200 kV in the bright-field image mode. A drop of the nanoparticles solution was cast on a 300-mesh carbon-coated copper grid and allowed to dry.

Electrophoretic mobilities of the bare Fe_3O_4 and coated Fe_3O_4 nanoparticles were measured using a zeta potential analyzer (Brookhaven Instruments, U.S.A).

Absorption spectra were recorded at room temperature on a Cary 100 UV−vis spectrophotometer.

Photoluminescence (PL) spectra data were obtained from an FS920 steady-state fluorescence spectrometer (Edinburgh Instruments) at room temperature. The excitation wavelength was selected at 400 nm.

Magnetization of the Fe_3O_4 nanoparticles was measured by a Quantum Design MPMS-XL SQUID magnetometer. The field dependence of the magnetization was studied over the range from −4 to +4 kOe at 298 K, in which the magnetization of the nanoparticles was totally saturated.

Results and Discussion

Multilayer structures of the magnetic luminescent nanocomposites, Fe_3O_4/PE_n/CdTe and $Fe_3O_4/(PE_3/CdTe)_n$, were fabricated as schematically outlined in Scheme 1. The Fe_3O_4 nanoparticles were used as the template. Their average size was about 8.5 nm, which was confirmed by TEM and XRD (see Supporting Information). They are negative in a basic medium since the magnetic hydrosol has an isoelectric point of 6.6.[40] Meanwhile, carboxyl groups of adipic acid adsorbed on the surface of the Fe_3O_4 nanoparticles were ionized in the Tris aqueous of pH 9.0 to enhance the negative charge of the surface and improve the stability of the nanoparticles. The large amount of surface negative charge was therefore favorable for the deposition of positively charged PAH. With driving of the electrostatic interactions, positively charged PAH or negatively charged PSS were alternatively deposited onto the surface of Fe_3O_4 nanoparticles, forming uniform polyelectrolyte multilayers. Based on that, the thickness of polyelectrolyte interlayer film could be tuned. It means that the distance between the Fe_3O_4 nanoparticles and the CdTe QDs could be well-adjusted. Additionally, the polyelectrolyte interlayers could provide a positively charged outer surface to facilitate the adsorption of the negatively charged QDs.[31,41] Furthermore, the CdTe QDs could also be repetitiously adsorbed onto the surface of the Fe_3O_4 nanoparticles with the help of the polyelectrolyte multilayers. In our experiment, all of the constituents to fabricate the nanocomposites dissolved in water, and therefore it provided the nanocomposites with fine water solubility, which laid the foundations of their success in biologic, clinical, and diagnostic applications.

Fe_3O_4/PE_n/CdTe Nanocomposites. Several experimental techniques can be employed to monitor the formation of each polyelectrolyte layer deposited sequentially on colloids. Microelectrophoresis provides a qualitative indication as to whether multilayers are deposited.[42,43] Figure 1 shows the ζ-potential as a function of polyelectrolyte layer number for negatively charged Fe_3O_4 nanoparticles coated with PAH and PSS. As expected, the original Fe_3O_4 nanoparticles had a negative ζ-potential of −25.7 mV. The presence of a

(40) Regazzoni, A. E.; Urrutia, G. A.; Blesa, M. A.; Maroto, A. J. G. *J. Inorg. Nucl. Chem.* **1981**, *43*, 1489.
(41) Caruso, F.; Spasova, M.; Susha, A.; Giersig, M.; Caruso, R. A. *Chem. Mater.* **2001**, *13*, 109.
(42) Donath, E.; Sukhorukov, G. B.; Caruso, F.; Kavis, S. A.; Möhwald, H. *Angew. Chem., Int. Ed.* **1998**, *37*, 2201.
(43) Caruso, F.; Donath, E.; Möhwald, H. *J. Phys. Chem. B* **1998**, *102*, 2011.

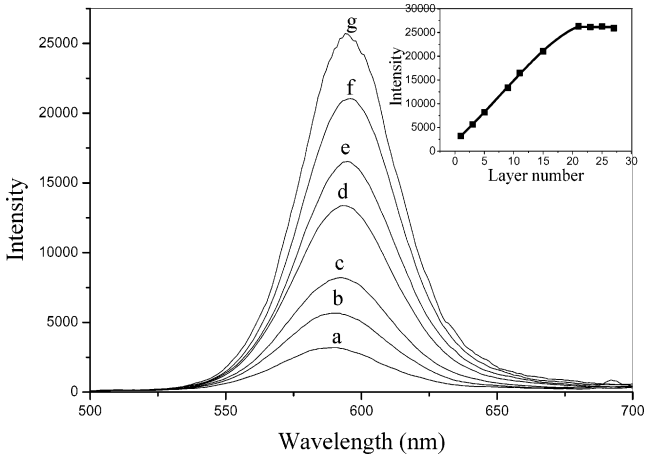

Figure 2. PL spectra of the magnetic luminescent nanocomposites $Fe_3O_4/PE_n/CdTe$. From a to g, $n = 1$, 3, 5, 9, 11, 15, and 21, respectively. The inset shows a plot of the PL intensity vs the number of deposition cycle.

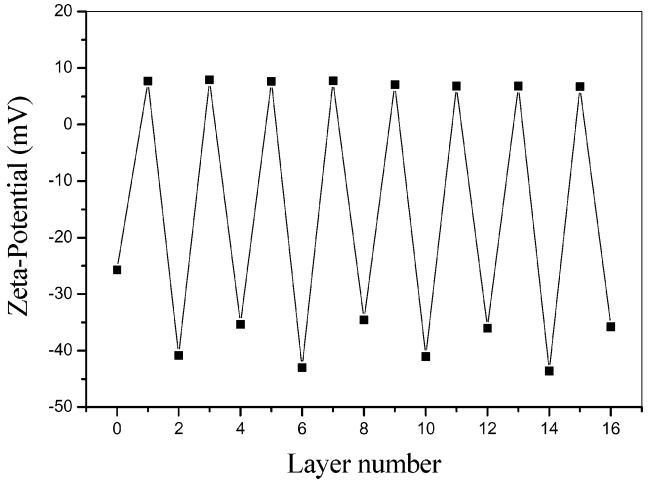

Figure 3. Zeta-potential of the magnetic luminescent nanocomposites $Fe_3O_4/PE_n/CdTe$. The odd layer number corresponds to PAH deposition, $(2n + 4)$ layer to PSS deposition, and the $4n$ layer to the CdTe QD deposition, where $n = 1$, 2, 3, and 4, respectively.

single layer of adsorbed positively charged PAH on the Fe_3O_4 nanoparticles caused a reversal in ζ-potential to positive values (+7.5 mV), and subsequent deposition of a negatively charged PSS reversed the ζ-potential back to negative values (−41.5 mV). Further polyelectrolyte depositions caused the ζ-potential to alternate in sign, depending on whether the outermost layer was positively or negatively charged. Deposition of the CdTe QDs onto PE_n-coated Fe_3O_4 nanoparticles with the outermost layer of PAH caused the ζ-potential to be reversed from +7 to −35 mV. This ζ-potential was lower than the one of PSS since the original CdTe QDs yielded a lower ζ-potential of about −38.1 mV while PSS yielded that of −44.3 mV. The alternation in ζ-potential qualitatively demonstrated a successful recharging of the particle surface with the deposition of each polyelectrolyte layer and the CdTe QDs and suggested the stepwise layer growth occurring during the fabrication of the magnetic luminescent nanocomposites.

The PL properties of $Fe_3O_4/PE_n/CdTe$ nanocomposites were investigated at the fixed concentration of coated Fe_3O_4 nanoparticles. Figure 2 shows the PL emission spectra of the nanocomposites with a different number of polyelectrolyte layers up to 27 layers. The narrow emission bands at about 595 nm were demonstrated. The PL intensity was very sensitive to the distance between the Fe_3O_4 nanoparticles and the CdTe QDs. It was enhanced with a corresponding increase of the thickness of polyelectrolyte interlayers and remained a constant maximum after 21 layers of polyelectrolytes. In the system, polyelectrolyte multilayers themselves did not influence the PL signal from the CdTe QDs.[32] Thus, the enhancement of PL might be caused by two other things. One was that, as a transition metal oxide, the interaction between the Fe_3O_4 and the QDs would lead to energy transfer, and hence influence the PL properties of the nanocomposites.[44] This kind of interaction was extremely sensitive to the separation distance between the Fe_3O_4 nanoparticles and the QDs and drastically diminished with the increasing of distance. The other was that the surface area of a single particle increased with adsorbed polyelectrolyte layers, leading much more CdTe QDs to deposit on the surface per unit of the Fe_3O_4 nanoparticles. However, this increase was confined to a certain region. When the finite magnitude was extended, it would lead to a decrease of PL due to quenching by the concentration. The influences on PL were considered to be a cooperative effect of the two factors, the distance and the concentration. They might reach approximative equilibrium after 21 polyelectrolyte layers are deposited.

$Fe_3O_4/(PE_3/CdTe)_n$ Nanocomposites. $Fe_3O_4/(PE_3/CdTe)_n$ nanocomposites were prepared by repetitious deposition of PE_3/CdTe on the Fe_3O_4 nanoparticles. The polyelectrolyte interlayers not only acted as molecular "glue" but they could also impart enhanced colloidal stability to the coated particles via electrostatic as well as steric contributions. The outermost layer was PAH, therefore providing a positively charged surface for CdTe QDs deposition.

One of the prerequisites for the sequential deposition of oppositely charged polyelectrolytes and the CdTe QDs onto the Fe_3O_4 nanoparticles was charge inversion at the end of each deposition step. Figure 3 shows the ζ-potential as a function of repetitiously adsorbed PE_3/CdTe QDs onto the Fe_3O_4 nanoparticles. The prime ζ-potential of the Fe_3O_4 nanoparticles was negative. After adsorbed PAH, it inversed to be positive. And the resulting positive surface charge allowed for coating with a layer of negatively charged PSS, followed by adsorption of PAH once more, and the ζ-potential inversed to be positive again. Subsequent deposition of the CdTe QDs onto PE_3-coated Fe_3O_4 would result in a negative ζ-potential.

Further evidence for the formation of the composites of $Fe_3O_4/(PE_3/CdTe\ QDs)_n$ was provided by UV−vis absorption spectra. Figure 4 shows the absorption spectra of the Fe_3O_4 nanoparticles, CdTe QDs, and the magnetic luminescent nanocomposites with one to four deposition cycles of PE_3/CdTe QDs on the Fe_3O_4 nanoparticles, respectively. The adsorption spectra of the Fe_3O_4 nanoparticles and CdTe QDs dispersions were retained in the magnetic luminescent nanocomposites, where the absorbance peak at about 560 nm was in agreement with the one of CdTe QDs in Figure 4c−f. It

(44) Agekyan, V. F. *Phys. Solid State* **2002**, *44*, 2013.

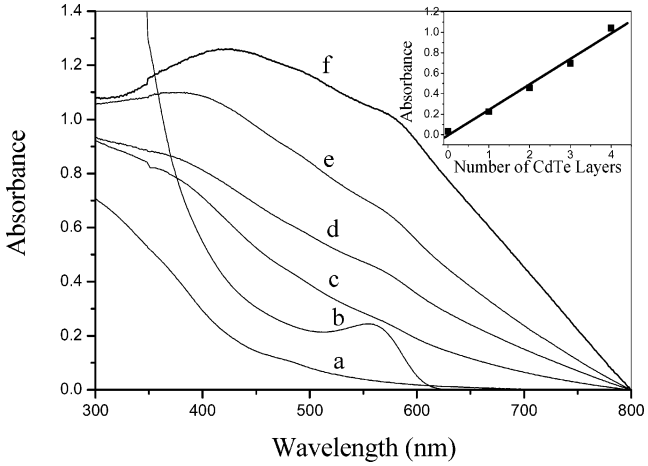

Figure 4. UV−vis spectra of (a) the Fe_3O_4 nanoparticles, (b) the CdTe QDs, and (c−f) the magnetic luminescent nanocomposites with different CdTe QDs deposition cycles. Curves c−f refer to Fe_3O_4/PE_3/CdTe, Fe_3O_4/(PE_3/CdTe)$_2$, Fe_3O_4/(PE_3/CdTe)$_3$, and Fe_3O_4/(PE_3/CdTe)$_4$, respectively. The inset shows a plot of the absorbance at 560 nm vs the number of the CdTe QD deposition layers.

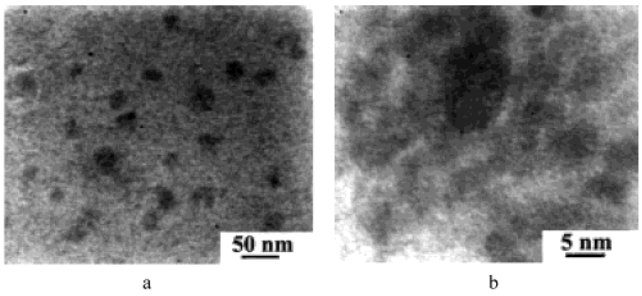

Figure 5. (a) A TEM image of the magnetic luminescent nanocomposites with three deposition cycles of CdTe QDs/PE_3 on the Fe_3O_4 nanoparticles. The average diameter of the composites was about 34 nm. (b) A high-resolution TEM image of a single magnetite nanoparticle coated with three layers of CdTe QDs/PE_3. It allowed visualization of the CdTe QDs with lower contrast adsorbed on the surface of a magnetite nanoparticle.

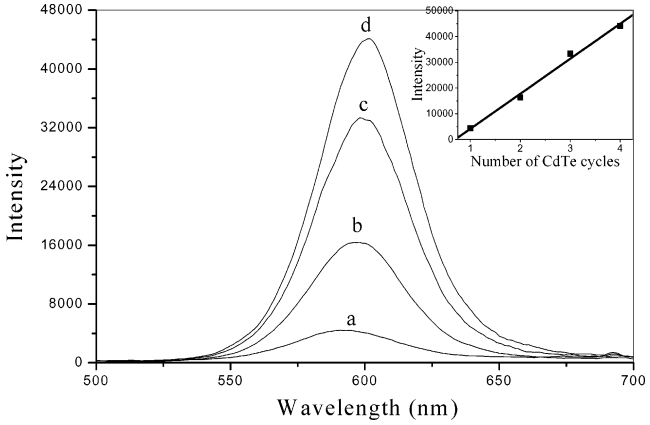

Figure 6. PL spectra of Fe_3O_4/(PE_3/CdTe)$_n$. The curves, from a to d, correspond to the number of deposition cycles *n* from 1 to 4. The inset shows the increase of PL intensity with the number of the CdTe QD deposition cycles.

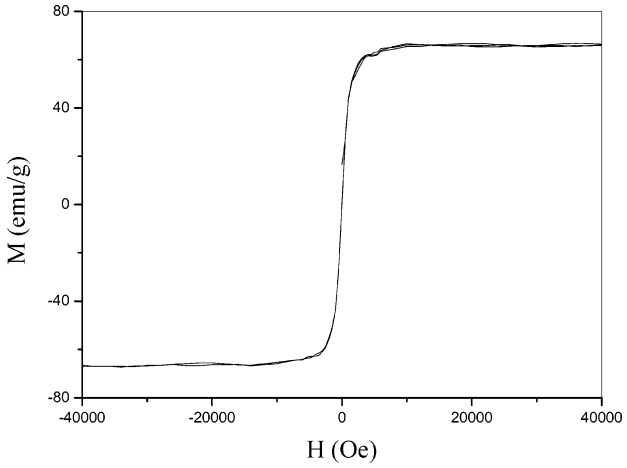

Figure 7. Magnetization curve of magnetite nanoparticles at room temperture. There was no hysteresis, i.e., no remanence or coercivity, which was consistent with superparamagnetic behavior.

illustrated that the CdTe QDs were assembled successfully into PE_3-coated Fe_3O_4 nanoparticles. The absorbance at 560 nm was used to monitor the efficiency of the LbL self-assembly process. The observed linear increase of the CdTe QDs absorbance vs the corresponding deposition number indicated a stepwise and uniform assembling process (shown in the inset in Figure 4).

Topography and the size of the magnetic luminescent nanocomposites could be directly visualized by TEM. Figure 5a shows the TEM image of Fe_3O_4/(PE_3/CdTe)$_3$. The average diameter of the composites was about 34 nm. Few aggregations were observed. A high-resolution TEM image of a single Fe_3O_4/(PE_3/CdTe)$_3$ nanocomposite is shown in Figure 5b. It was obvious that the CdTe QDs with lower contrast were adsorbed on the surface of the Fe_3O_4 nanoparticle. Because the components of the polyelectrolytes in the nanocomposites had too low electron density to contribute to the contrast in the image, only gaps between the QDs and the Fe_3O_4 nanoparticles could be observed.

For the single magnetic luminescent nanocomposite, the concentration of the CdTe QDs could also be adjusted by varying the deposition cycles of the PE_3/CdTe QDs multilayers. This adjustment would influence the PL of the nanocomposites and finally resulted in the increase of PL within the finite range (Figure 6). In our experiments, the relative emission intensity of the composite was linearly enhanced with the increase of CdTe QDs deposition cycles (the insert in Figure 6).

Rapid Magnetic Separation of the Magnetic Luminescent Nanocomposites. Rapid efficient collection and accurate sensitive detection of various water-soluble bioconjugates have become one of the desired scientific goals with ramifications in immunoassay, bioseparation, and biolabeling applications. However, it is difficult for the conventional QDs-labeled bioconjugate materials, even under ultracentrifugation conditions. The magnetic luminescent nanocomposites overcame this disadvantage due to their magnetic property derived from the Fe_3O_4 nanoparticles. Figure 7 shows the magnetization loop of the Fe_3O_4 nanoparticles at 298 K. The curve was free of any hysteresis and the zero coercivity was obvious, which were consistent with superparamagnetic behavior and the nanoscale dimensions of the particles. The superparamagentic property meant that the nanoparticles were magnetic only when placed in a very strong magnetic field. Removed the magnetic field, it would lead to a rapid decay of the

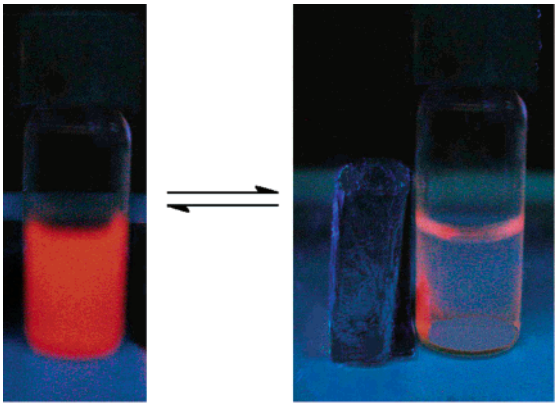

Figure 8. Photograph images of the magnetic luminescent nanocomposites under UV irradiation (a) without and (b) with an external magnetic field. The magnetic field strength of the magnet was 1000 G. A color change from the orange to transparent was observed when an external magnetic field was applied, showing the aggregation processes. The aggregations could be dispersed rapidly when the magnetic field was removed.

magnetization. It is critical for the magnetic luminescent nanocomposites to succeed as labels for separation or bioassay. If the individual particle possessed a remnant magnetic field, each particle would act as a small dipole magnet, resulting in aggregations and precipitation of the particles. Figure 8 illustrates the separation and redispersion process of the magnetic luminescent nanocomposites. In the absence of an external field, the dispersion of the magnetic luminescent nanocomposites was orange and homogeneous under UV radiation (Figure 8a). When the external magnetic field was applied, magnetic luminescent nanocomposites were enriched and the dispersion became clear and transparent (Figure 8b). With removal of the magnetic field followed by vigorous stirring, the aggregations were rapidly redispersed. It should be mentioned that the magnetic properties of the nanocomposites also made it possible for site-specific transport.

Conclusion

In this paper, we presented a LbL assembly approach to fabricate the water-soluble magnetic luminescent nanocomposites. The Fe_3O_4 nanoparticles were used as a template for the controlled adsorption of CdTe QDs/polyelectrolyte multilayers. With variation of the number of deposition cycles of polyelectrolyte interlayers and CdTe QDs/polyelectrolyte multilayers, the nanocomposites of $Fe_3O_4/PE_n/CdTe$ and $Fe_3O_4/(PE_3/CdTe)_n$ were successfully fabricated, respectively. It was found that the controlled distance of the polyelectrolyte interlayer between the magentic nanoparticles and QDs and the CdTe QDs loading on the nanocomposites played a key role in improving the PL of the nanocomposites. Besides the intensive PL, the nanocomposites simultaneously exhibited excellent magnetic properties and were easily separated from solution using a permanent magnet. In a few words, the PL, magnetic, and water-soluble properties of the nanocomposites would allow them to find a large range of applications for biolabeling, bioseparation, immunoassay, and diagnostics.

Acknowledgment. The work was supported in part by grants from “863”, “973” projects and the National Natural Science Foundation of China. We are grateful to Dr. Song He from the University of Hong Kong, China, for valuable discussions.

Supporting Information Available: TEM image and XRD patterns of the Fe_3O_4 nanoparticles (PDF). This material is available free of charge via the Internet at http://pubs.acs.org.

CM049422O